RSC Advances

Dynamic Article Links

Cite this: *RSC Advances*, 2012, **2**, 1769–1773

www.rsc.org/advances

COMMUNICATION

Three-dimensional hierarchically structured PAN@γ–AlOOH fiber films based on a fiber templated hydrothermal route and their recyclable strong Cr(VI)-removal performance†

Yongxing Lin, Weiping Cai,* Hui He, Xianbiao Wang and Guozhong Wang

Received 21st October 2011, Accepted 11th December 2011
DOI: 10.1039/c2ra00945e

A simple route is presented to fabricate a polymer (polyacrylonitrile, PAN)@γ –AlOOH composite fiber film, with a three-dimensional hierarchical micro/nanostructure, based on electrospun fiber templated hydrothermal strategy. The composite fibers are nest-like in morphology and consist of cross-linked γ–AlOOH nanoplates, with 20 nm–40 nm of thickness, standing nearly vertically on the PAN fibers. The formation of such composite fibers are attributed to the template-induced heterogeneous growth of γ–AlOOH on the PAN fibers in alkaline conditions. Further, such fibers can be converted into the tubular Al_2O_3 hollow fibers with the nearly unchanged morphology after calcination in air. Importantly, the as-prepared PAN@γ–AlOOH composite fibers have shown a much higher adsorption capacity than the normal γ–AlOOH nanopowders, and especially, exhibited very good recycling performance (more than 85% of its original adsorption capacity after 4 cycles), as an adsorbent to remove the heavy metal ions, Cr(VI), from model wastewater. This material could thus serve as an effective recyclable adsorbent with easy separation from solution. Also, it is expected to have other potential applications in the role of a sensitive material or catalyst.

It is well known that some nanosized materials could be used as effective adsorbents of heavy metals or other contaminants and may play an important role in water purification.[1–3] However, there are some vital defects hindering the practical applications of powdered nano-adsorbents. Firstly, the agglomeration of nanoparticles, which deprives the nanomaterials of their characteristics and excellent properties, takes place in almost every occasion. Secondly, the collection after use not only increases the difficulties in separation from solution but also defeats any chance of recycling the material. For instance, the isolation of the powdered nanomaterials from solution through centrifugation complicates the operation process and is highly inconvenient for recycling. Moreover, residues can result from the above treatment such as sludge, which is always a difficult issue because of their potential toxicity, and can add to the contamination problems of the environment after they enter the surroundings.[4] As an alternative approach to avoid agglomeration, inorganic hierarchically micro/nanostructured materials or the microsized objects with nanostructures, such as dandelion-like CuO[5] and ZnO,[6] flower-like iron oxide[7] and γ–AlOOH,[8] and hierarchical MnO,[9] have been successfully prepared. These materials are of the steady activity due to their structural geometry. However, separation is still a challenge owing to their existence in the form of powders.

It is well known that polymer is a kind of excellent recyclable materials with good elasticity and pliability.[10] Recently, electrospun polymer fiber mats (or films) have exhibited great potential in environmental remediation because they are freestanding and recycled easily and can also be integrated onto another matrix conveniently.[11–13] Also, the fibers possess several attractive advantages, such as a comparatively low cost, applicability to various materials and the ability to generate relatively large-scale integrated film, which are very important in practical applications.[14] Obviously, if the micro/nanostructured inorganic materials grow on the electrospun polymer fibers' surface, a flexible composite fiber film would be formed with 3 dimensional (3D) micro/nanostructures. Such a structured composite material is expected to possess both the advantages of polymer fibers and micro/nanostructured inorganic materials, and hence overcome the above shortcomings of the powdered nanomaterials, which has been confirmed in our recent work.

In this communication, a simple route is presented to fabricate the polymer (polyacrylonitrile, PAN) @γ–AlOOH composite fibers, based on an electrospun fiber templated hydrothermal strategy. In this strategy, the electrospun PAN fibers are used as a flexible template. Nanostructured γ–AlOOH grows on the fibers' surface, forming three-dimensional (3D) micro/nanostructured composite fibers *via* a subsequent hydrothermal route. Here, the electro-spun PAN fibers are directly used as the substrate of γ–AlOOH growth and can also be used as the sacrificial template to build the micro/nanostructured hollow or tubular inorganic fibers, as illustrated in Scheme 1. Using such a route, we have obtained 3D PAN@γ–AlOOH micro/nanostructured flexible material, which consists of cross-linked γ–AlOOH nanoplates which are nearly vertically standing on the PAN fibers and with 20–40 nm in thickness. Such fibers can be converted into tubular Al_2O_3 hollow fibers with nearly

Key Lab of Materials Physics, Anhui Key Lab of Nanomaterials and Nanotechnology, Institute of Solid State Physics, Chinese Academy of Sciences, Hefei, 230031, P. R. China. E-mail: wpcai@issp.ac.cn

† Electronic supplementary information (ESI) available: Experimental details, the histogram of the fibers' diameter, FESEM images (S2–S4), the fitting plots according to Freundlich model. See DOI: 10.1039/c2ra00945e

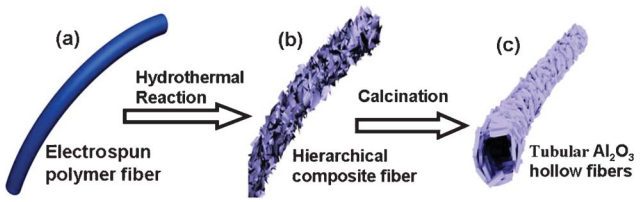

Scheme 1 Schematic illustration for fabrication of the polymer@γ–AlOOH composite fibers with a 3D micro/nanostructure. (a): an electrospun polymer fiber. (b): the composite fiber after the electrospun fiber templated hydrothermal reaction. (c): a tubular hollow fiber after calcination of the composite fiber.

unchanged morphology after calcination in air. Importantly, the as-prepared PAN@γ–AlOOH fibers have shown much higher adsorption capacity than the normal γ–AlOOH nanopowders, and in particular, exhibited very good recycling performance (more than 85% of their original adsorption capacity after 4 cycles), as an adsorbent to remove the heavy metal ions, Cr(VI), from model wastewater. This material could thus serve as an effective recyclable adsorbent with easy separation from solution. Also, it is expected to have other potential applications such as sensitive material or catalyst. The details are reported in the following.

PAN fiber was first prepared by electrospinning, as previously described.[14] Briefly, 5 ml dimethylformamide (DMF) solution of PAN (8% wt, MW ~ 60 000) was put into a syringe with an internal hole diameter of 0.7 millimetre. The inject rate of the solution was controlled to be about 0.1 ml h^{-1}. The electrospinning was carried out on a homemade electrospinning apparatus. The fibers were collected on a rotatable drum to form a piece of net-like film. After that, 0.01 g of the as-prepared PAN fiber film and 1.5 g of aluminium powder were mixed together in 40 ml hexamethylenetetramine ($C_6H_{12}N_4$, or HMTA for short) aqueous solution (1% wt), and transferred into a Teflon autoclave and heated to a temperature of 110 °C for 10 h before cooling to the room temperature. The pH value of the solution increases from 7.5 initially to 10 after reaction. The mixture of the fibers and the powders was then taken out and washed with deionized water, and finally dried in a vacuum oven at 50 °C for 24 h.

The inset in Fig. 1A shows a photo of the freestanding electrospun PAN fiber film, which is about 60 mm × 60 mm and white in color. Scanning electron microscopic (SEM) observation has revealed that the film consists of fibers, which are randomly arranged and form a net-like porous film, as shown in Fig. 1A. Most of fibers fall into the range from 200 nm to 400 nm in diameter, as illustrated in Fig. S1, ESI†. After hydrothermal reaction, the film is unchanged in color. But X-ray diffraction (XRD) measurement shows that the phase constitution, before and after reaction, is different, as illustrated in Fig. 1B. The peaks at 17° and 27° correspond to those of the PAN fibers.[15] After reaction, the new peaks can be clearly identified as orthorhombic γ–AlOOH (JCPDS card 21-1307), indicating formation of PAN@γ–AlOOH. Fig. 1C presents a typical SEM image for the sample after reaction, showing the PAN@γ–AlOOH fibers, which are much thicker than the pure PAN fibers (about 600 nm ~ 1 μm in diameter). We can see that the products are homogeneously distributed on the fibers. Local magnification has revealed that the products are cross-linked γ–AlOOH nanoplates nearly vertically standing on the fibers, exhibiting the 3D nest-like nanoarchitecture, as shown in Fig. 1D. The nanoplates are 80–150 nm in edge size and 15 ~ 40 nm in thickness (see the inset in Fig. 1D).

Transmission electron microscopic (TEM) examination was also conducted. Fig. 2A shows the morphology corresponding to a segment of the composite fiber. The selected area electron diffraction (SAED) pattern of a nanoplate, which is perpendicular to the electron beam, shows that the nanoplate is single crystal with planar orientation [0$\bar{1}$1], as illustrated in Fig. 2B and its insets. In addition,

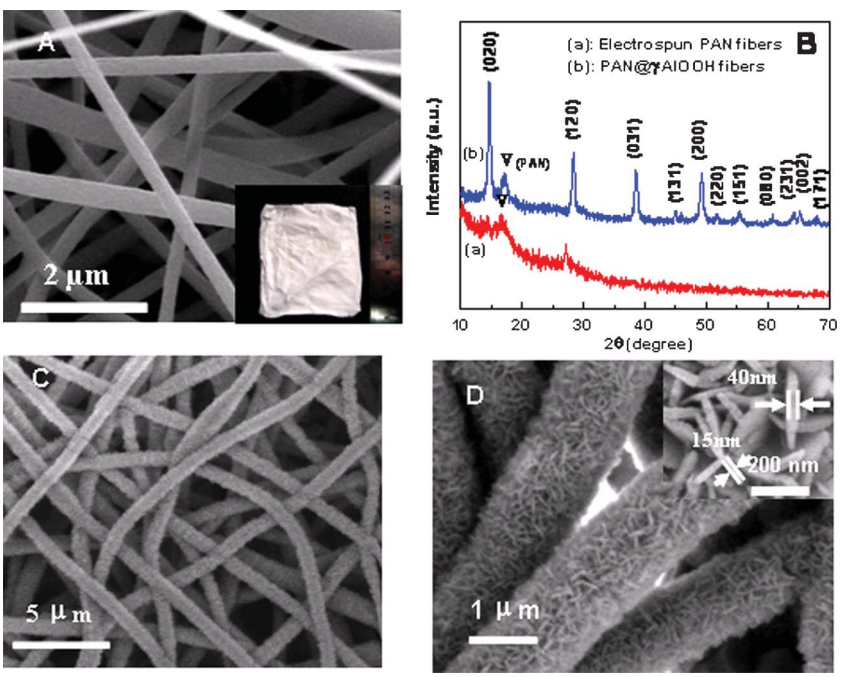

Fig. 1 (A) FESEM image of electrospun PAN fibers; The inset is a photo of the fiber film. (B) XRD patterns of electrospun PAN fibers (a) and the PAN@γ–AlOOH composite fibers (b); (C) FESEM image of the PAN@γ–AlOOH composite fibers. (D) a local magnified image of (C), the inset is a further magnified image.

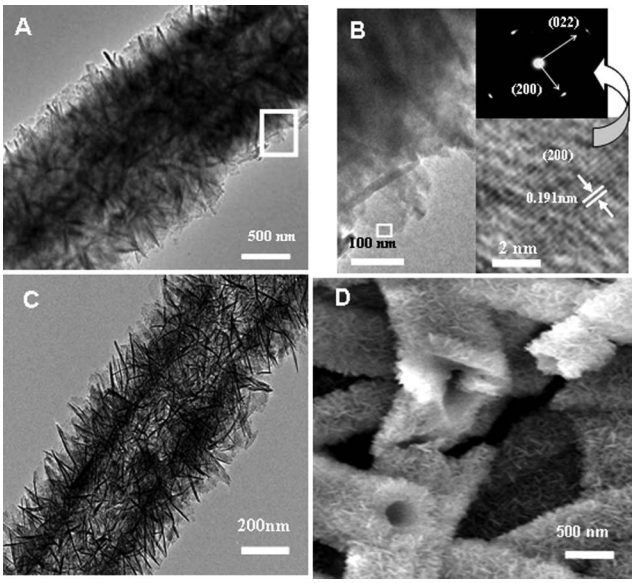

Fig. 2 Microstructural examination of the prepared composite fibers. (A) TEM image of a single as-prepared PAN@γ–AlOOH fiber. (B) A local magnified image corresponding to the rectangular area marked in (A); The down-right inset: a high resolution TEM image corresponding to the rectangular area marked in (B); Up-right inset: the selected area electron diffraction pattern of a nanoplate vertical to the electron beam. (C) TEM image of a single PAN@γ–AlOOH after calcination at 550 °C, showing a tubular hollow structure. (D) FESEM image corresponding to the sample in (C).

based on the isothermal nitrogen sorption measurement and the Brunauer–Emmett–Teller (BET) equation,[16] the specific surface area of the composite fibers was evaluated to be about 19 $m^2\ g^{-1}$. Further, the AlOOH content in the composite fibers were estimated to be 47.4 wt%, by the difference in the film-weight before and after the hydrothermal reaction. So, the specific surface area of the cross-linked γ–AlOOH nanoplates in the composite fibers should be about 40 $m^2\ g^{-1}$. It should be mentioned that such composite fiber film still keeps its flexibility. Also, if the composite fibers were subsequently calcined at 550 °C in air, the PAN fibers would be thus burned away, and hollow or tubular hierarchical micro/nanostructured fibers could be obtained, as shown in Fig. 2C and D, corresponding to the TEM and SEM observations, respectively. The nanoplates are still vertically standing and cross-linked, but the PAN fibers have been removed and a tubular hollow structure is left. According to the previous reports,[17–19] the phase transformation, from boehmite to alumina, takes place in the temperature range from 250 °C to 550 °C. So the obtained hollow fibers should be Al_2O_3. Such structured materials could be used as catalysts[20] or catalyst supports.[21–23]

Further experiments have indicated that the reaction duration and concentration of $C_6H_{12}N_4$ (or HMTA) in the precursor solution are important to promote the formation of the above PAN@γ–AlOOH micro/nanostructured fibers. When the reaction time is short (say, 3 h), there are only very few ultrafine nanoplates formed and standing on the PAN fibers (Fig. S2A, ESI†). Increasing the reaction time leads to more and bigger nanoplates. Fig. S2B, ESI† shows the results corresponding to a 6h reaction. Much more nanoplates are observed on the fibers. Only if the reaction is long enough (say, 10 h), can we obtain the cross-linked and dense nanoplates homogeneously and nearly vertically standing on the fibers (Fig. 1C and D).

Also, HMTA in the precursor solution played a key role in formation of the nanoplates during the hydrothermal reaction. When its concentration is low (say, 0.1% wt), only few nanoplates form on the PAN fibers (Fig. S3A, ESI†). Increasing the concentration (say, 0.25% wt) leads to more nanoplates (Fig. S3B). However, if the concentration is too high (say, 10% wt), the reaction products are the mixture of the big particles (about 300 nm in size) and floc, which densely surround the fibers (Figs. S3C, D). Only an appropriate concentration (say, 1% wt) can induce the cross-linked γ–AlOOH nanoplates nearly vertically standing on the fibers with 3D nest-like micro/nanoarchitecture (Fig. 1C and D).

Here the formation of the 3D nest-like micro/nanoarchitectured PAN@AlOOH can be briefly described below. When the precursor solution with PAN fibers and metallic aluminum was heated at 110 °C, the following reactions would take place:

$$C_6H_{12}N_4 + 6H_2O \rightarrow 6HCHO + 4NH_3 \quad (1)$$

$$NH_3 + H_2O \rightarrow NH_4^+ + OH^- \quad (2)$$

$$Al + 2H_2O + OH^- \rightarrow Al(OH)_4^- + H_2 \quad (3)$$

$$Al(OH)_4^- \rightarrow AlOOH + H_2O + OH^- \quad (4)$$

Firstly, HTMA or $C_6H_{12}N_4$ reacts with water and produces ammonia [reaction (1)].[24–25] Then ammonia in turn hydrolyzes and the OH^- ions are generated, which makes the solution alkaline (or pH value increases) [reaction (2)]. Secondly, in such a basic solution, with $C_6H_{12}N_4$ hydrolysis going on, aluminum atoms would react with excessive hydroxyl ions and form $Al(OH)_4^-$[26–29] [reaction (3)], which in turn decompose and transform into AlOOH in hydrothermal conditions[30–31] [reaction (4)]. When the concentration of AlOOH is saturated, γ–AlOOH nuclei would be formed on the PAN fibers.

It has been reported that the appropriate basic conditions favor formation of 2D γ–AlOOH nanosheets,[26,30,32] which is a layered structure with an octahedral arrangement within the lamellae, and hydroxyl ions hold the lamellae together through hydrogen bonding.[33,34] Under acidic conditions, the solution contains protons, which combine with the hydroxyl oxygen lone pairs to give aqua ligands and destroy the γ–AlOOH layers, the separated layers subsequently curl into a 1D nanostructure *via* the scrolling-growth route. In reverse, the 2D lamellar structure would be retained in basic solution.[35] In this study, the initial reaction solution was weakly basic with a pH above 8. The plate-like γ–AlOOH nuclei would preferentially grow along the [100] and [011] directions within the plane($0\bar{1}1$). Only the (200)-oriented γ–AlOOH nuclei can grow continuously and the other oriented nuclei cannot sufficiently grow due to the geometric limitation. Finally, with the reaction, the cross-linked γ–AlOOH nanoplates are formed nearly vertically standing on the fibers, exhibiting the 3D nest-like micro/nanoarchitecture (see Fig. 1D).

As for the effect of HTMA in the precursor solution on the morphology of products, it is easy to understand based on the reactions (1, 2, 3). The low concentration of HTMA corresponds to the low OH^- concentration, which will produce less $Al(OH)_4^-$ ions and only slowly form the products [reactions (3, 4)], leading to the few γ–AlOOH within the same reaction time (see Fig. S3 A, B, ESI†), while too high a concentration of HTMA, corresponding to high OH^- concentration, will induce the fast formation of γ–AlOOH, resulting in densely distributed products with irregular morphology.

Importantly, the as-prepared PAN@γ–AlOOH composite fibers shown in Fig. 1c, which are convenient to collect and separate from solution, can be used as efficient adsorbents for the removal of Cr(VI) from solution with good reusability. Here, the adsorption capacity of γ–AlOOH (containing 47.4 wt% in the composite fibers) is employed to represent that of the composite fibers since pure PAN cannot remove Cr in the solution.[14]

The adsorption isotherm of Cr(VI) ions (pH = 3) on the as-prepared PAN@γ–AlOOH composite fibers shown in Fig.1C, is illustrated in curve (a) of Fig. 3A, which shows a much stronger adsorption than the γ–AlOOH nanopowders (32 m^2 g^{-1} in specific surface area) [curve (a_0) of Fig. 3A], prepared according to the route previously described[36] (See the morphology shown in Fig S4, ESI†). Quantitatively, the adsorption isotherms of Cr(VI) ions on the composite fiber and the powders follow the Freundlich model very well,[37] as shown in Fig S5†. Furthermore, the adsorption capacity of the composite fibers depends on the pH value of the Cr(VI)-contained solution, and decreases with rising pH value [see curves (a, b, c) in Fig. 3A]. Here, it should be mentioned that adsorption treatment induces increase of pH value of the solution slightly rises.

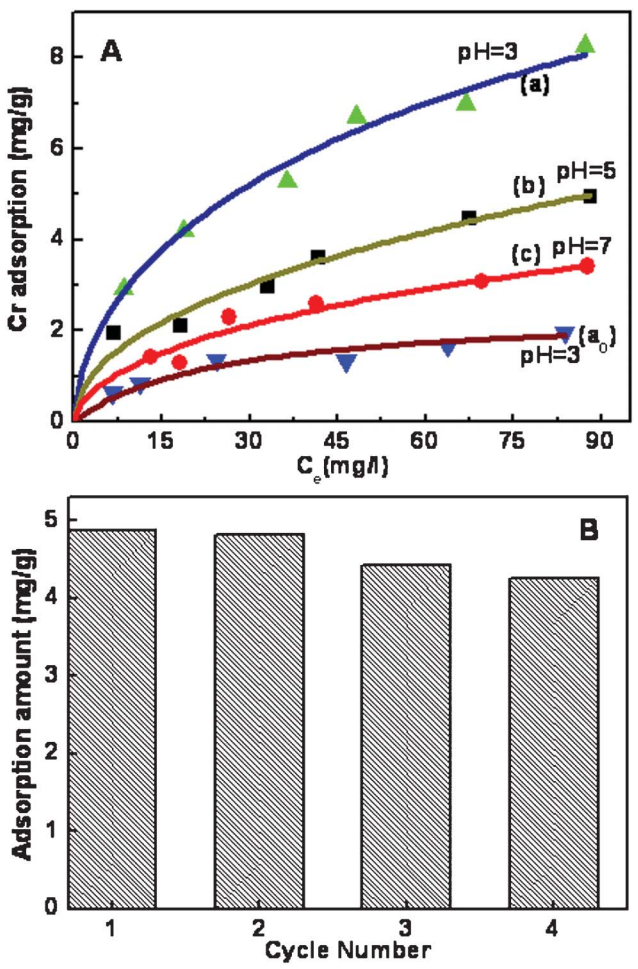

Fig. 3 (A) Adsorption isotherms of γ–AlOOH nanopowders (a_0) and the PAN@γ–AlOOH composite fibers (a, b, c) at different pH values. Solid lines: fitting results according to Freundlich model.[37] (B) The cycled adsorption capacity of PAN@γ–AlOOH fiber to Cr(VI) in cycled adsorption/desorption experiments at pH = 3.

More importantly, such hierarchically structured PAN@γ–AlOOH fibers have exhibited a stable recycling adsorption ability. Fig. 3(B) shows such a recycling adsorption capacity for the composite fibers, in Cr(VI) solution with pH = 3, washed by 0.01 M NaOH (details are described in the ESI†). The PAN@γ–AlOOH fibers still retained more than 85% of its original Cr(VI)-adsorption capacity after four cycles, demonstrating the stable recycling adsorption ability.

The high adsorption capacity for the hierarchically structured PAN@γ–AlOOH fibers can mainly be attributed to their special structure. Furthermore, since the cross-linked γ–AlOOH nanoplates nearly vertically standing on the fibers are of high structural stability, they would prevent the morphology from breaking down during recycling experiments, and keep the high active surface area, showing good cycling performance. Importantly, different to powdered adsorbents, which should be separated by centrifugation after remediation, our composite fibers can be simply collected and reclaimed by tweezers after an experiment.

As for the pH-value dependent adsorption capacity, it could be attributed to the surface protonation of the adsorbent (γ–AlOOH) in acidic solution. At a low pH value, the γ–AlOOH surface is highly protonated and hence favors adsorption of Cr(VI) ions which mainly exist in the form of $HCrO_4^-$.[38]. The surface protonation degree should reduce with an increase in pH-value, leading to a decrease of adsorption capacity [see curves (a, b, c) in Fig.3A]. In addition, the protonation is a proton-consuming reaction and should increase the pH values of the solution.[39] This has been confirmed in our experiment. Typically, the pH value increases to 4.2 after adsorption for the solution with initial pH = 3 in our case.

In summary, the PAN@γ–AlOOH composite fibers, with 3D hierarchical micro/nanostructure, have been fabricated for the first time by a simple route, based on electrospun fiber templated hydrothermal strategy. The formation of the composite fibers can be attributed to template-induced heterogeneous growth of γ–AlOOH on the PAN fibers in alkaline conditions. Owing to the structural geometry of the composite fibers, the tubular Al_2O_3 hollow fibers with the nearly unchanged morphology can be obtained after removal of the PAN fiber by calcination in air. More importantly, due to the 3D miro/nanostructure-induced stability against aggregation, the PAN@γ–AlOOH composite fibers are of a much higher adsorption capacity than conventional γ–AlOOH nanopowders as an adsorbent to remove the heavy metal ions, Cr(VI), from solution. This material could serve as a candidate adsorbent for environment remediation because of its effective recyclable performance and easy separation from solution. Also, it is expected to have other potential applications such as a role as a sensitive material or catalyst.

Acknowledgements

This work was financially supported by the National Basic Research Program of China (Grant No 2007CB936604).

References

1 J. Theron, J. A. Walker and T.E. Cloete, *Crit. Rev. Microbiol.*, 2008, **34**, 43–69.
2 N. Savage and M. S. Diallo, *J. Nanopart. Res.*, 2005, **7**, 331–342.
3 J. Y. Bottero, J. Rose and M. R. Wiesner, *Integr. Environ. Assess. Manage.*, 2006, **2**, 391–395.
4 M. A. Shannon, P. W. Bohn, M. Elimelech, J. G. Georgiadis, B. J. Marinas and A. M. Mayes, *Nature*, 2008, **452**, 301–310.
5 B. Liu and H. C. Zeng, *J. Am. Chem. Soc.*, 2004, **126**, 8124–8125.

6 B. Liu and H. C. Zeng, *J. Am. Chem. Soc.*, 2004, **126**, 16744–16746.
7 L. S. Zhong, J. S. Hu, H. P. Liang, A. M. Cao, W. G. Song and L. J. Wan, *Adv. Mater.*, 2006, **18**, 2426–2431.
8 J. Zhang, S. Liu, J. Lin, H. Song, J. Luo, E. M. Elssfah, E. Ammar, Y. Huang, X. Ding, J. Gao, S. Qi and C. Tang, *J. Phys. Chem. B*, 2006, **110**, 14249–14252.
9 Z. Li, Y. Ding, Y. Xiong, Q. Yang and Y. Xie, *Chem. Commun.*, 2005, **7**, 918–920.
10 C. D. Craver and C. E. Carraher, *Applied Polymer Science: 21st Century*, 2000, Elsevier B.V., ISBN: 978-0-08-043417-9.
11 H. Ma, K. Yoon, L. Rong, Y. Mao, Z. Mo, D. Fang, Z. Hollander, J. Gaiteri, B. S. Hsiao and B. Chu, *J. Mater. Chem.*, 2010, **20**, 4692–4704.
12 Y. Yoon, B. S. Hsiao and B. Chu, *J. Membr. Sci.*, 2009, **338**, 145–152.
13 K. Yoon, K. Kim, X. F. Wang, D. F. Fang, B. S. Hsiao and B. Chu, *Polymer*, 2006, **47**(7), 2434–2441.
14 Y. X. Lin, W. P. Cai, X.Y. Tian, X. L. Liu, G. Z. Wang and C. H. Liang, *J. Mater. Chem.*, 2011, **21**, 991–997.
15 R. B. Mathura, O. P. Bahla, J. Mittala and K. C. Nagpal, *Carbon*, 1991, **29**, 1059–1061.
16 S. Brunauer, P. H. Emmett and E. Teller, *J. Am. Chem. Soc.*, 1938, **60**, 309–319.
17 J. T. Kloprogge, H. D. Ruan and R. L. Frost, *J. Mater. Sci.*, 2002, **37**, 1121–1129.
18 C. P. Lin and S. B. Wen, *J. Am. Ceram. Soc.*, 2002, **85**, 1467–1472.
19 E. Suvaci, G. Simkovich and G. L. Messing, *J. Am. Ceram. Soc.*, 2000, **83**, 299–305.
20 C. Ma, Y. Chang, W. Ye, W. Shang and C. Wang, *J. Colloid Interface Sci.*, 2008, **317**, 148–154.
21 K. Pattamakomsan, E. Ehret, F. Morfin, P. Gelin, Y. Jugnet, S. Prakash, J. C. Bertolini, J. Panpranot and F. J. C. S. Aires, *Catal. Today*, 2011, **164**, 28–33.
22 M. S. Gong, J. U. Kim and J. G. Kim, *Sens.Actuators, B*, 2010, **147**, 539–547.
23 B. M. Venkatesan, B. Dorvel, S. Yemenicioglu, N. Watkins, I. Petrov and R. Bashir, *Adv. Mater.*, 2009, **21**, 2771–2776.
24 Z. Xia, J. Sha, Y. Fang, Y. Wan, Z. Wang and Y. Wang, *Cryst. Growth Des.*, 2010, **10**, 2759–2765.
25 K. Govender, D. S. Boyle, P. B. Kenway and P. O'Brien, *J. Mater. Chem.*, 2004, **14**, 2575–2591.
26 X. Y. Chen, H. S. Huh and S. W. Lee, *Nanotechnology*, 2007, **18**, 285608–2856012.
27 H. Liang, L. Liu, Z. Yang and Y. Yang, *Cryst. Res. Technol.*, 2010, **45**, 195–198.
28 Z. P. Xu and G. Q. Lu, *Chem. Mater.*, 2005, **17**, 1055–1062.
29 C. Feng, Q. Wei, S. Wang, B. Shi and H. Tang, *Colloids Surf., A*, 2007, **303**, 241–248.
30 S. Zanganeh, A. Kajbafvala, N. Zanganeh, M. S. Mohajerani, A. Lak, M. R. Bayati, H. R. Zargar and S. K. Sadrnezhaad, *Appl. Phys. A: Mater. Sci. Process.*, 2010, **99**, 317–321.
31 P. Benezeth, D. A. Palmer and D. J. Wesolowski, *Geochim. Cosmochim. Acta*, 2008, **72**, 2429–2453.
32 W. Cai, J. Yu and M. Jaroniec, *J. Mater. Chem.*, 2010, **20**, 4587–4594.
33 H. W. Hou, Y. Xie, Q. Yang, Q. X. Guo and C. R. Tan, *Nanotechnology*, 2005, **16**, 741–745.
34 X. Bokhimi, J. A. Toledo-Antonio, M. L. Guzman-Castillo and F. Hernandez-Beltran, *J. Solid State Chem.*, 2001, **159**, 32–40.
35 X. Y. Chen and S. W. Lee, *Chem. Phys. Lett.*, 2007, **438**, 279–284.
36 Y. Q. Wang, G. Z. Wang, H. Q. Wang, W. P. Cai, C. H. Liang and L. D. Zhang, *Nanotechnology*, 2009, **20**, 155604–155609.
37 H. Freundlich, W. Heller, Rubber die adsorption in lusungen, *J. Am. Chem. Soc.*, 1939, **61**, 2228–2230.
38 K. Selvi, S. Pattabhi and K. Kadirvelu, *Bioresour. Technol.*, 2001, **80**, 87–89.
39 S. Mor, K. Ravindra and N. R. Bishnoi, *Bioresour. Technol.*, 2007, **98**, 954–957.